Ionic film deposition from single-filament dielectric-barrier discharges – Comparison of hexamethyldisiloxane and hexamethyldisilane precursors

L. Bröcker[1], N. Steppan[1], K. Hain[2], T. Winzer[3], J. Benedikt[3], M. Stankov[4], D. Loffhagen[4] and C.-P. Klages[1]

[1] *Institute for Surface Technology (IOT), Technische Universität Braunschweig, Braunschweig, Germany*
[2] *Fraunhofer Institute for Surface Engineering and Thin Films, Braunschweig, Germany*
[3] *Institute of Experimental and Applied Physics, Faculty of Mathematics and Natural Sciences, Kiel, Germany*
[4] *Leibniz Institute for Plasma Science and Technology (INP), Greifswald, Germany*

Abstract: Single-filament dielectric-barrier discharges at atmospheric pressure are used to investigate the effect of short residence times on the plasma polymerization of hexamethyldisiloxane (HMDSO) and hexamethyldisilane (HMDS), respectively. Experiments with precursor fractions between 25 and 2000 ppm in argon show that neither radicals are deposited nor surface reactions with the monomer take place. Possible pathways for the ionic deposition using HMDSO or HMDS are discussed.

Keywords: Ionic deposition, DBD, single-filament, PECVD, hexamethyldisilane, HMDSO

1. Introduction

Thin film deposition using dielectric-barrier discharges at atmospheric pressure is barely understood. Especially the share of film forming ions, radicals, or surface reactions of the monomer with reactive surface sites in the overall deposited mass is currently not known. Therefore, in a first step, it would be of great interest to isolate one of the three named deposition mechanisms to (i) simplify models of relevant physical and chemical reactions and to (ii) possibly develop completely new plasma polymer films.

Generally, a carrier gas is needed at atmospheric pressure to transport the often liquid monomer into the discharge zone. In the here reported experiments, we used relatively small molar fractions $25 \leq x_M$ / ppm ≤ 2000 of hexamethyldisiloxane [HMDSO, $(CH_3)_3Si\text{-}O\text{-}Si(CH_3)_3$] or hexamethyldisilane [HMDS, $(CH_3)_3Si\text{-}Si(CH_3)_3$] in argon 6.0. It is worth to mention that the choice of the carrier gas strongly affects the plasma-physical and -chemical processes. Contrary to thermal chemical vapour deposition (CVD), plasma-enhanced CVD (PECVD) includes processes where collisions of Ar atoms in resonant or metastable Ar(1s) states and the Ar_2 excimers with the monomer lead to Penning ionization (PI) as well as to dissociation into neutral radicals. Excitation energies of Ar(1s) states range between 11.55 and 11.83 eV [1] and the argon excimers have energies of approximately 9.8 eV [2]. Loffhagen et al. have shown that for HMDSO fractions up to 200 ppm PI processes are the dominant electron source and contribute 90 % of the total ionization rate [3]. Even for monomer fractions reaching 1500 ppm, PI still contributes 63 % [4].

Results shown in this contribution were obtained with an asymmetric single-filament dielectric-barrier discharge (SF-DBD) setup: A tungsten tip electrode glued onto borosilicate glass forms the high voltage (HV) electrode and a silicon wafer on the reactor bottom made from aluminum forms the ground. Due to the small radial dimensions of the HV electrode, the plasma dimensions in gas flow direction are always around 1 mm or below. It has to be mentioned that "single-filament" does not mean that a filamentary discharge is observed, quite the contrary an atmospheric-pressure glow discharge (APGD) is present, but that there is only one localized current pulse for every charge reversal. Single-filament DBDs are of substantial interest, because small plasma dimensions result in low gas residence times $t_{res} = l_{plasma}/v_{av}$. Here, v_{av} represents the average gas flow velocity in the discharge zone and l_{plasma} is the plasma extension in gas flow direction. With v_{av} = 50 cm/s and l_{plasma} = 0.1 cm, t_{res} is only 2 ms. Conventional DBDs with electrode lengths of about 10 cm have t_{res} = 200 ms. The residence time is a key parameter in relation to the diffusion time of film forming radicals t_{diff} and the ion drift time t_{drift}. Ions reach the surface in microsecond and neutrals need tens to hundreds of milliseconds [5]. Therefore, using a SF-DBD setup, radicals are transported out of the plasma zone and only ions formed from the monomer are deposited in the plasma region.

It is important to note that independent of the underlying ionization mechanism, a molecular ion is formed at first [6]. The appearance energy of possible fragment ions as well as the ionization cross section and rate coefficient for the decay, respectively, determine the abundance of the deposited ions. In case of HMDSO, it is well known that PI processes as well as electron impact ionization lead mainly to the production of the pentamethyldisiloxanyl ion [$PMDSO^+$, $(CH_3)_3Si\text{-}O\text{-}Si^+(CH_3)_2$] and a methyl radical ($CH_3$). Jiao et al. have shown that the ionization cross section for electron energies between 10 and 100 eV is always the highest for the decay into $PMDSO^+$ and CH_3 [7]. Other fragment ions are almost negligible. In case of HMDS, it is much more difficult to make a statement about which ions are formed and deposited, especially at atmospheric pressure. Rate coefficients for the decay into a trimethylsilyl cation [$TriMS^+$, $(CH_3)_3Si^+$] and a trimethylsilyl radical [TriMS, $(CH_3)_3Si$] as well as into a pentamethyldisilanyl ion [$PMDS^+$, $(CH_3)_3Si\text{-}Si^+(CH_3)_2$] and CH_3 are below the frequency for collisional stabilisation of the parent ion $HMDS^+$ of about 10^9 s^{-1} [8]. A comparison of both monomers is particularly interesting due to different gas phase and surface processes.

In the present study, we report on experimental data from thin film characterization as well as the electrical characterization of our SF-DBD setup using different concentrations of HMDSO and HMDS in argon. For

structural analysis, we used Fourier-transform infrared (FTIR) spectroscopy in attenuated total reflection (ATR), Raman spectroscopy, and wavelength-dispersive X-ray spectroscopy (WDXS). To get an idea about the mass of deposited ions, profilometry measurements were compared with the calculated mass from the transferred charge, obtained by electrical measurements. Additionally, mass spectrometry measurements were performed with a nearly identical DBD setup to interpret the experimental results.

2. DBD setup

The asymmetric SF-DBD setup for thin film deposition is shown in Fig. 1. A tungsten tip electrode glued with epoxy resin onto a 1.1 mm thick borosilicate dielectric forms the HV electrode and the bottom of the reactor made from aluminum forms the ground. Acetone-cleaned silicon wafer pieces with a length of 2 cm and a width of 1 cm are placed on the reactor bottom below the HV electrode resulting in a discharge gap of 2.5 mm. Liquid HMDSO and HMDS, respectively, were filled in a glass bubbler and transported with an argon stream into the discharge zone. A second argon stream served for diluting and adjusting the monomer fraction. An oscilloscope was used to (i) monitor the applied voltage U_{a0}, which was adjusted to 1.75 kV ± 0.05 kV, and (ii) to monitor the voltage over a 1 nF capacitor in series to the DBD setup to calculate discharge currents, the dissipated energy and the transferred charge per period. For all experiments, an operating frequency of 19 kHz and v_{av} = 50 cm/s were used. The oxygen concentration in the discharge zone was always below 1 ppm.

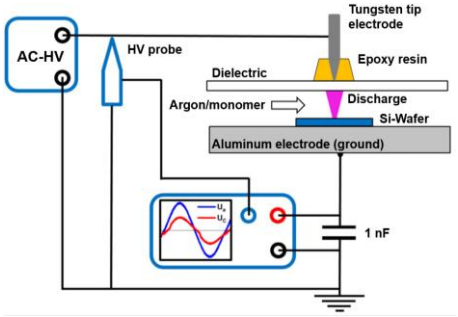

Fig. 1. SF-DBD setup

3. Results

Electrical characteristics and photographs taken of the plasma are very similar and indicative of the Penning effect for both monomers. Fig. 2 shows, on the left, photographs of the plasma for 100 ppm and 2000 ppm HMDS in Ar, respectively, and, on the right, the ignition voltage $U_{a0,Ig}$ and extinction voltage $U_{a0,Ex}$ over the monomer fraction x_M. $U_{a0,Ig}$ ($U_{a0,Ex}$) is the applied voltage U_{a0} resulting in ignition (extinction) when U_{a0} is slowly increased (lowered). Besides an overall diffuse plasma appearance, a rapid decline of $U_{a0,Ig}$ and $U_{a0,Ex}$ with growing monomer fractions is observed, up to about 250 ppm. Then a slow increase of both voltages is found.

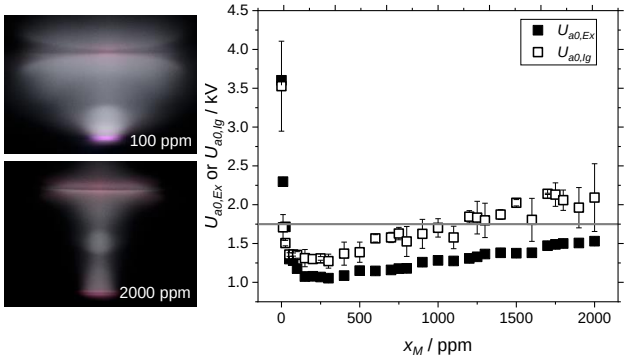

Fig. 2. Photographs taken of the plasma for 100 ppm and 2000 ppm HMDS (left), and ignition $U_{a0,Ig}$ and extinction $U_{a0,Ex}$ voltage over the monomer fraction (right)

The trends for both voltage curves seen in Fig. 2 resemble spark voltages reported by Heylen who investigated the Penning effect of different hydrocarbons in argon [9].

To calculate the average deposited ion mass M_{Ion}, at first the volume per transferred charge V_q in cm³/mol was determined. Therefore, profilometric line scans through the center of the deposits in gas flow direction and across are performed. Fig. 3 shows a deposit from 1000 ppm HMDS in argon on the left and a line scan on the right. Due to virtual circular symmetry, numerical integration of these line scans results in the deposited volume V_p. Dividing by the number of transferred elementary charges from electrical measurements, V_q is determined. With respect to the density of the plasma polymer and the sticking coefficient of the deposited ions a value for M_{Ion} can be estimated, see chapter 4.

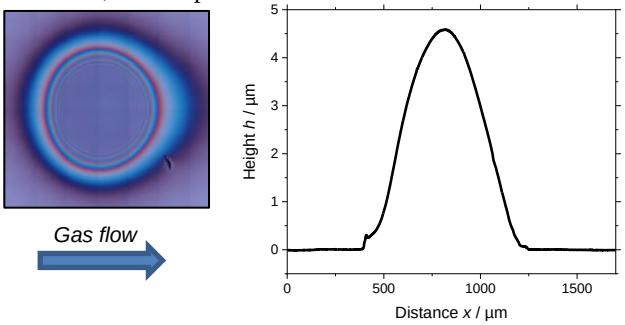

Fig. 3. Picture of a deposit from 1000 ppm HMDS (left) and profilometric line scan (right)

Fig. 4 shows values for the calculated volume per elementary charge V_q over the concentration range for HMDSO and HMDS. With growing monomer fraction, trends for both monomers are at first characterized by a constant value for V_q (≈ 140 cm³/mol for HMDSO and ≈ 110 cm³/mol for HMDS) and a subsequent increase, starting at approximately x_M = 250 ppm for HMDS and 1000 ppm for HMDSO. V_q nearly doubles for HMDSO and triples for HMDS, indicating an ionic oligomerization process. It is worth mentioning that by discharge pulsing with varying plasma-off and maintaining plasma-on times,

the same volume per charge is deposited. Reducing the gap by 60 % leads to the same V_q, too.

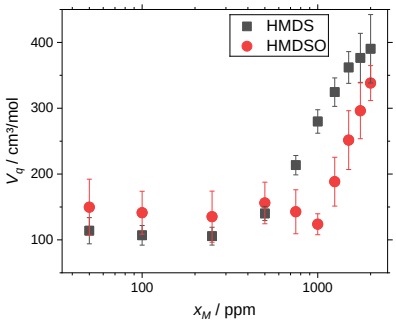

Fig. 4. Volume per elementary charge V_q for HMDSO (red) and HMDS (black) fractions from 50 to 2000 ppm

Fig. 5 shows FTIR-ATR spectra for experiments with 2000 ppm HMDSO (red line) and 2000 ppm HMDS (black line) in argon, respectively. Interestingly, there are nearly no structural changes when the monomer fraction is varied, indicating that always the same structural elements are incorporated. This applies for both HMDSO and HMDS.

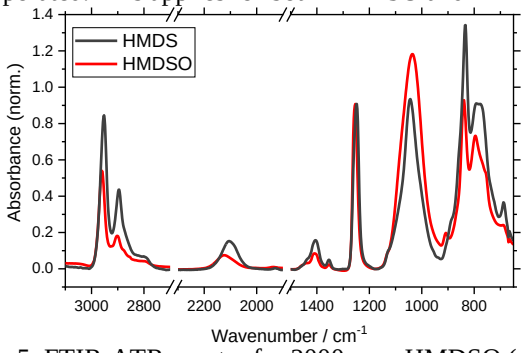

Fig. 5. FTIR-ATR spectra for 2000 ppm HMDSO (red line) and HMDS (black line). Data was normalized to the bending vibration of CH_3 in $Si(CH_3)_x$ at 1250 cm^{-1}

Plasma polymers made from HMDS show more intense methyl vibrations around 3000 cm^{-1}, 1405 cm^{-1} and below 840 cm^{-1}, respectively. Especially trimethyl-substituted silicon is more present, indicating a lesser degree of crosslinking in such polymers. Additionally, the band at approximately 1050 cm^{-1} is an indicator for the occurrence of Si-O-Si and Si-CH_2-Si: A broader and larger peak indicates a larger amount of Si-O-Si whereas a smaller and thinner peak indicates that Si-CH_2-Si is mostly present. In case of HMDS the signal at 1050 cm^{-1} is much more defined and smaller than for HMDSO. Therefore, we conclude that the backbone of plasma polymers made from HMDS consists mostly of Si-CH_2-Si structural elements and the backbone of HMDSO of Si-O-Si. Raman measurements do not show Si-Si signals for any plasma polymer.

WDXS analysis allows to correlate the elemental composition of possible film-forming ions with the plasma polymer. Fig. 6 shows the [C/Si] and [O/Si] ratios for thin films made from HMDSO. Besides the elemental composition of the plasma polymers, it also includes the elemental composition of possible ions obtained by ionic oligomerization (dotted line: $Me_3SiOSiMe_2OSi^+Me_2$, heptamethyltrisiloxanyl cation, $HMTSO^+$ with 221 amu; dashed line: $Me_3SiO(SiMe_2O)_2Si^+Me_2$, nonamethyltetrasiloxanyl cation, $NMTSO^+$ with 295 amu). The decrease of the [C/Si] ratio with increasing monomer fraction is in good agreement with an increase of relevant oligomer cations. In case of HMDS, the elemental composition does not change over the monomer fraction and is always [C/Si] ≈ 3 and [O/Si] ≈ 0.2.

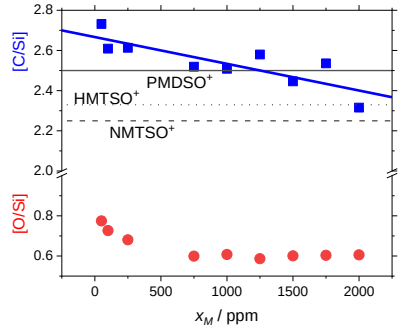

Fig. 6. Atomic percent ratios [C/Si] and [O/Si] for different x_M of HMDSO. Horizontal lines indicate possible oligomer ions; see text for more information

To support the experimental results, mass spectrometry measurements were performed using a DBD setup which was very similar to the one in Fig. 1. The setup was placed in such a way, that the orifice of the mass spectrometer was always near the first visible interference ring (cf. Fig. 3), because the deposition rate was too high in the center of the deposit. It has to be mentioned that the share of photoionization due to UV radiation from the plasma is possibly quite high and the share of ions formed due to PI processes or electron impact ionization differs strongly from the here-mentioned data. Due to the complexity of the mass spectra for different monomer fractions of HMDS and HMDSO in argon, the most important insights are summarized here: For x_M < 1000 ppm of HMDSO, the most prominent peak is always $PMDSO^+$ with 147.3 amu at a percentage of around 75 % or more. For larger x_M, the most intense peak is assigned to a cation with a mass of 309 amu, indicating a relatively abrupt onset of ionic oligomerization. In case of HMDS in argon, the $HMDS^+$ monomer cation with a mass of 146.4 amu is always the dominant peak with a percentage around 90 % or more.

4. Discussion

Plasma polymerization using the SF-DBD (cf. Fig. 1) indicates an ionic deposition mechanism and the occurrence of the Penning effect. Nearly perfect circular symmetry of the thin films and the same volume per transferred charge for reduced gap heights or longer plasma-off times are strong indicators for the sole deposition of ions. Reduced gap heights would lead to an increased deposition of radicals due to lower diffusion times whereas reactions of the monomer with surface radicals can take place during plasma-off times.

The relevance of the Penning effect is reflected in the generally diffuse appearance of the discharge as well as in the ignition and extinction voltage, respectively. A strong decline for x_M up to 250 ppm indicates an effective electron production and therefore earlier ignition due to PI processes. The reason for the increase of $U_{a0,Ig}$ and $U_{a0,Ex}$ respectively, for larger x_M is currently under investigation.

In order to determine the average deposited ion mass, values for the density ρ of the plasma polymers and the sticking coefficient η have to be assumed. For plasma-polymerized HMDSO (pp-HMDSO) as well as pp-HMDS a value of 1.1 g/cm³ was chosen which equals the density of pp-HMDSO films at low pressure and relatively low power [10] as well as thin films deposited from tetramethylsilane that structurally resemble plasma polymers made from HMDS at similar low-pressure and low-power conditions [11]. The mass accommodation coefficient η formally resembles a low-pressure sticking coefficient as known from surface physics. Here, $\eta = 1$ was chosen as an effect of the small free path length in a DBD running at 1 bar. Fig. 7 shows the calculated average deposited ion mass M_{Ion} for HMDSO and HMDS in argon in dependence on the monomer fraction.

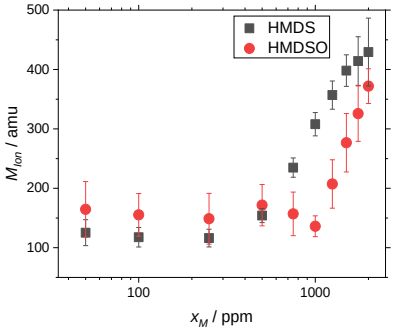

Fig. 7. Calculated average ion mass M_{Ion} for HMDSO (red) and HMDS (black) fractions up to 2000 ppm

The trends for both monomers are quite similar and especially the calculated average ion mass of HMDSO is in good agreement with mass spectrometry data as well as WDXS measurements. At first, a constant ion mass of about 150 amu is determined. For concentrations exceeding 1000 ppm, M_{Ion} increases up to 370 amu for 2000 ppm. A decrease in the [C/Si] ratio (cf. Fig. 6) as well as mass spectrometry measurements that show an abrupt rise for an ion with 309 amu supports these results. Therefore, mostly $PMDSO^+$ is deposited for lower x_M and ionic oligomerization takes place for x_M > 1000 ppm, where $PMDSO^+$ with a mass of 147.3 amu is added to HMDSO with a mass of 162.4 amu, leading to an ion with 309.7 amu. This process was reported in [12] for a low-pressure environment, too. FTIR-ATR analyses show typical structural elements of these ions, too, like Si-O-Si, di- and trimethyl-substituted silicon.

The calculated average deposited ion mass for HMDS in argon has a constant value of $M_{Ion} \approx 115$ amu for smaller monomer fractions. For x_M > 250 ppm, an increase up to 430 amu at 2000 ppm is found. Mass spectrometry data indicate a nearly exclusive production of the parent ion $HMDS^+$ and only negligible percentages of other ions, although M_{Ion} more than triples. When $HMDS^+$ reaches the surface, it is very likely that the cation takes up an electron whereby unreactive HMDS can be produced. Therefore, it is possible that processes in the plasma differ from those during mass spectrometry measurements where cations are probably primarily produced by 9.8-eV UV radiation: Energy transfer from Ar(1s) atoms with > 11.5 eV to HMDS can result in TriMS and $TriMS^+$, the latter being known to react quite rapidly with different monomers [13].

5. Conclusion

Single-filament DBDs at atmospheric pressure and small admixtures of HMDSO and HMDS in argon, respectively, have been studied using electrical measurements, FTIR-ATR and Raman spectroscopy, WDXS, profilometry and mass spectrometry. It is shown that film deposition is due to ionic species: For HMDSO, $PMDSO^+$ is deposited at monomer fractions up to 1000 ppm while for larger x_M ionic oligomers prevail. For HMDS, it is currently quite difficult to say which ions are formed, deposited and incorporated into the film. A detailed analysis will be part of future studies.

6. Acknowledgements

The work is funded by the Deutsche Forschungsgemeinschaft (DFG, German Research Foundation) – project number 504701852. The authors thank Meret Betz and Axel Pregizer-Winter from IOT as well as Prof. Dr. Ronny Brandenburg and Dr. Markus M. Becker from INP for helpful discussions. They also thank Cornelia Steinberg for performing the elemental analysis.

7. References

[1] L. Minnhagen, J. Opt. Soc. Am. **63**, 1185 (1973).
[2] U. Kogelschatz, J. Opt. Technol. **79**, 484 (2012).
[3] D. Loffhagen, et al., Contrib. Plasma. Phys. **58**, 1900169 (2018).
[4] D. Loffhagen et al., Plasma Process Polym. **17**, 1 (2020).
[5] F. Massines et al., Plasma Process Polym. **9**, 1041 (2012).
[6] J. H. Gross, *Mass Spectrometry*, 3rd edition, Springer, Cham (2017).
[7] C. Q. Jiao et al., Vac. Sci. Technol. A **23**, 1295 (2005).
[8] J. Z. Dávalos and T. Baer, J. Phys. Chem. A **110**, 8572 (2006).
[9] A. E. D. Heylen, Int. J. Electron. **30**, 121 (1971).
[10] L. Agres et al., J. Appl. Polym. Sci. **61**, 2015 (1996).
[11] Y. Catherine and A. Zamouche, Plasma Chem. Plasma Process. **5**, 353 (1985).
[12] M. R. Alexander et al., Plasmas Polym. **2**, 277 (1997).
[13] J. A. Stone, Res. Chem. Intermed. **16**, 257 (1991).